Structural Geology (The Journal of the Tectonic Research Group of Japan), No. 44, 47–57, 2000

Diffusion-controlled garnet growth during Sambagawa metamorphism

Mitsuhiro Toriumi* and Akiko Nomizo**

Abstract : Garnet from higher grade zones of the Sambagawa metamorphic belt commonly shows reverse zoning of MnO in the final stages of growth. The reverse zoning formed during growth process rather than by resorption. The magnitude of reverse zoning increases with increasing grain size. Given that grain size is proportional to linear growth velocity, a model of reverse zoning and growth velocity requires average compositions of chlorite different from equilibrium compositions. The model presented here is derived from competition of diffusive mass transfer of component ions of garnet in the matrix and interface migration due to garnet growth. This can well explain the occurrence of garnet cluster and relationships between the magnitude of reverse zoning and grain size.

Key words : *garnet, grain growth, diffusion, Sambagawa*

Introduction

Compositional zoning of garnet in medium to high grade metamorphic rocks can be used to infer P-T-t paths of metamorphism (e.g. Spear & Peacock, 1989 ; Vance & O'Nions, 1992). Garnet zoning in pelitic schists of the greenschist to amphibolite facies grade has been interpreted to result from continuous growth accompanied by an increase of temperature, or by Rayleigh type fractionation during a constant temperature (Hollister, 1966). Fractionation, however, is unable to produce the systematic change in the Fe-Mg partitioning between garnet and chlorite from early to late stage growth of garnet. The former model, on the other hand, allows us to interpret P-T paths by means of the metamorphic inversion method (Spear & Peacock, 1989).

Tracy (1982), St-Onge (1987) and Spear & Peacock (1989) developed modeling of garnet growth together with the sliding equilibrium and proposed a metamorphic inversion method which provides a quantitative and continuous P-T record, of metamorphism in a single rock. Their method for inversion is based on surface equilibrium and growth zoning due to P-T change. During the period of garnet growth, diffusion of component ions is very fast in the matrix relative to the growth velocity and then enrichment of Mn in the matrix at the growth front never occurs. In the above model, compositional zoning explicitly represents a record of P-T-t.

Hollister (1966), Kretz (1973) and Banno & Chii (1978) proposed models of garnet growth interpreting the Bell-shape zoning of MnO. In their models, reverse zoning of MnO is due to growth during retrograde metamorphism. Sakai et al. (1986) clarified growth zoning of garnet by means of back scattered electron images, and show two images which indicate growth and resorption. The electron images showing the resorption of garnet display growth outlines cross-cutting the inner contour lines of MnO and FeO contents.

On the contrary, crystal size distributions of garnet from low to high grade regional metamorphic rocks of the Appalachian belt in Maine were measured by Cashman & Ferry (1988) and from high pressure type regional metamorphic rocks of Kyushu, Japan by Miyazaki (1991). They attributed coarsening mechanism of garnet to Ostwald ripening during metamor-

Received 10 October 2000 ; accepted 15 November 2000
* Department of Complexity Science and Engineering, Graduate School of Frontier Sciences, University of Tokyo, Hongo, Bunkyo-ku, Tokyo
** Medical School of Juntenndo University Hospital, Hongo, Tokyo

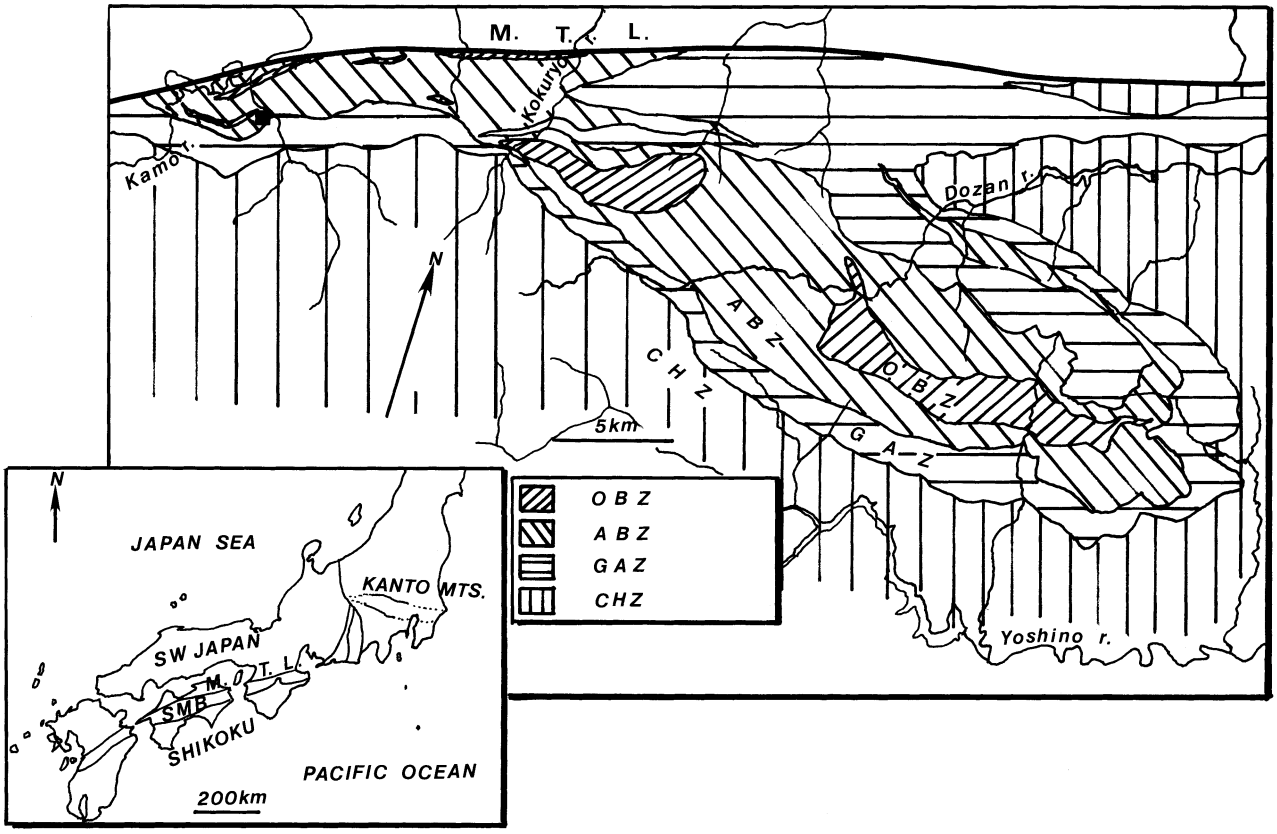

Fig. 1 Index and zonal maps of the Sambagawa metamorphic belt in Shikoku, SW Japan. The study area is shown by the closed square in the western part of the map. MTL ; Median tectonic Line, SMB ; Sambagawa metamorphic belt, OBZ ; oligoclase-biotite zone, ABZ ; albite-biotite zone, GAZ ; garnet zone, CHZ ; chlorite zone.

phism because the cyrstal size distributions are similar to an LSW type pattern. However, Ostwald ripening requires reduction in size of small grains rather than growth of large grains and does not depend on the diffusive mass transfer of component ions in the matrix. Nevertheless there is no evidence for the preferential resorption of small grains of garnet in metamorphic rocks (Toriumi, 1975), suggesting a growth process of garnet other than Ostwald ripening.

Kretz (1974) and Banno & Chii (1978) proposed that reverse zoning (MnO enrichment in the rim) is formed by the resorption of garnet. However, reversely zoned garnet grains formed by continuous growth are common in the Sambagawa metamorphic belt (Nomizo, 1989). Furthermore, Nomizo clarified that the compositional range of reverse zoning depend strongly on the grain size of garnet. Such reverse zoning requires a chemical gradient from the equilibrium interface to the matrix and consequenctly the diffusive mass transfer. In this paper, we propose a model of garnet growth that involves an advancing garnet-matrix interface competing with diffusion of constituent ions in the matrix. The ratio of growth velocity and diffusion rate of ions through chlorite in the matrix controls the degree of reverse zoning garnet growth.

Outline of the Sambagawa metamorphic belt

The samples have been collected from the Sambagawa metamorphic belt in central Shikoku, Japan. Sambagawa metamorphism occurred from 70 to 110 Ma, by means of K-Ar (Itaya & Takasugi 1988) and Ar-Ar method (Takasu & Dallemeyer, 1990). The peak metamorphism at about 600℃ and 15 kb occured at 110 Ma and retrograde metamorphism through 300℃ and 5–7 kb at 70 Ma. Thus the cooling rate is estimated to be >10℃/million years.

The Sambagawa metamorphism is a high pressure intermediate type regional metamorphism of pumpellyite-actinolite facies, glaucophane schist facies, and epidote amphibolite facies (e.g. Toriumi, 1990). The detailed spatial distribu-

tion of metamorphic zones has been clarified by the distribution of garnet, biotite and oligoclase-bearing assemblages in chemically homogeneous pelitic schists (Kurata & Banno, 1974 ; Higashino, 1990). The isothermal surfaces defined by the garnet, biotite and oligoclase-biotite isograds are penetratively folded with a southward vergence. Toriumi (1990) and Wallis (1991) postulated that the large penetrative fold of isothermal surfaces is attributed to a sheath fold of 5 km NS width and with an EW kinematic flow direction.

Recently, Nomizo (1992) suggested that the highest grade of the Sambagawa metamorphic belt reaches eclogite facies conditions. The physical conditions of Sambagawa metamorphism in the eclogite facies are thus estimated at 600–700℃ and 15–20 kb, and the epidote amphibolite facies conditions are inferred to be 500–600℃ and 10–15 kb (Takasu, 1989). The P-T paths of high grade rocks were traced near the adiabatic depression, suggesting rapid uplift process relative to thermal diffusion. Retrograde metamorphism is widely recognized in the Sambagawa metamorphic belt as chlorite formation after garnet in pelitic schists and actinolite formation in pull-apart structure within hornblende.

Intense plastic deformation during metamorphism occurred with an E-W transport direction (Faure, 1983 ; Toriumi, 1982, 1986, 1990). Faure pointed out that synmetamorphic ductile deformation of the Sambagawa belt is represented by top-to-east shear sense, although Wallis (1991) documented top-to-west sense of the ductile shear in central Shikoku. Further, Mori (1986) and Toriumi (1989) suggested that the metamorphic belt is divided into many domains having top-to-the east and top-to-the west shear sense, and concluded inhomogeneous ductile shear during Sambagawa metamorphism. Late stage deformation during retrograde metamorphism resulted in the displacement of the thermal structure defined by the surface of the isograd, and is thought to be represented by the NS vergent pile nappe structure of thrust sheets (Hara et al., 1990). However, many retrograde cracks sealed by quartz and calcite record E-W extension and our data suggest that metamorphic isograds are not cut by thrusts as proposed by Hara et al. (1990). This indicates that no large NS displacement by thrusts can be found.

Mineral assemblages of pelitic schists of the chlorite zone, the garnet zone, the albite-biotite zone and the oligoclase-biotite zone are chlorite, chlorite-garnet, chlorite-garnet-biotite, and chlorite-garnet-biotite-oligoclase together with albite and quartz, respectively. During Sambagawa metamorphism, the divariant reaction producing garnet across the garnet zone is as follows,

$$\text{chlorite} + \text{quartz} = \text{garnet} + H_2O$$

Thus, the isograd defined by this equation requires constant XFe in chlorite (and the bulk rock). With increasing metamorphic grade, the volume fraction of chlorite decreases and that of garnet increases in zones higher than the garnet zone. The Mg/Fe ratio in chlorite increases with increasing metamorphic grade (Higashino, 1990). In the biotite zone, the reaction proposed above involves muscovite in the left and biotite in the right hand side, because of the appearence of biotite. However, Kurata & Banno (1974) and Banno & Sakai (1990) obtained gradual increase of the partition coefficients of FeO and MgO between garnet and chlorite and gradual increase of MgO and decrease of MnO content in garnet from the garnet zone to the oligoclase-biotite zone. Thus it is concluded that the metamorphic temperature increases gradually from the garnet zone to the oligoclase-biotite zone and that the change from the divariant to the univariant reaction does not control the reverse zoning of MnO content in garnet growth. Basic rocks show a systematic change of mineral assemblages with increasing metamorphic temperature from the pumpellyite zone, pumpellyite-chlorite zone, pumpellyite-actinolite zone, barroisite zone, and the hornblende zone (Otsuki & Banno, 1990).

Experimental procedures

The analysed samples were obtained from the albite-biotite zone in the Saijo district in central Shikoku, as shown in Fig. 1. Detailed sampling points are shown in Fig. 2. The mineral assemblages of pelitic schists and basic schists are garnet-muscovite-albite-biotite-ilmenite-quartz-calcite and hornblende-chlorite-garnet-albite-

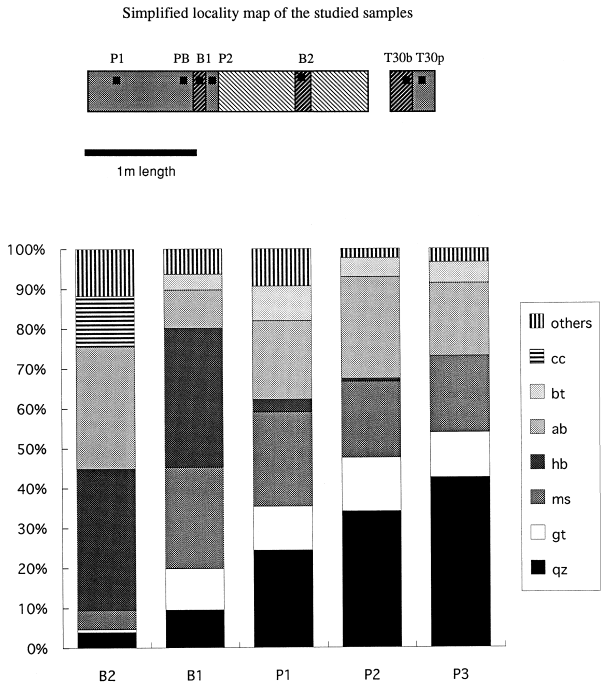

Fig. 2 Relative sample location of studied pelitic and basic schists in the locality shown in Fig. 1., samples P1to B2 are the same as those denoted by q36 in Table 1. The distance between B2 and T30b is 3 meters. The mineral composi- tions of the samples are shown in (b). Qz ; quartz, Ga ; garnet, Ms ; muscovite, Ab ; albite, Bt ; biotite, Hb ; hornblende, Cc ; calcite.

quartz-muscovite, respectively. Volume fractions of these minerals are shown in Fig. 2. The size of garnet varies largely from 0.1 to 10 mm. Volume fractions of garnet are ranged from 5 to 10 percents.

Crystal size frequency distributions (CSD) of garnet were measured using an optical microscope. The total number of grains in schists having large grain of garnet is 196 from two 10 cm×10 cm wide thin sections. CSDs of micaceous and quartz-albite layers were also measured to clarify the effect of mineral compositions. Local means of grain spacing and grain size were calculated as the mean of 5 grains.

The microprobe analyses and Xray composition mappings of garnet and chlorite were carried out by a JEOL XMA type 8600 the University of Tokyo, and partial analyses of bulk compositions of pelitic and basic schists were performed by XRF at the Geological Institute, University of Tokyo.

Grain size distribution of garnet

Garnet displays a commonly euhedral outline. Two types of microstructures are apparent porphyroblastic grains containing abundant mineral inclusions, and small grains containing small numbers of inclusions. Although there is a great difference of the mean grain size, the pattern of the crystal size frequency distribution of garnet is very similar in both porphyroblastic and small garnet bearing pelitic schists (Fig. 3). The CSD function is approximated to be a LSW type except for large grain size region but not lognormal type as shown by Cashman & Ferry (1988), Miyazaki (1991) and Toriumi (1975), and they attributed the CSD pattern to Ostwald ripening during coarsening of garnet grains. The figure 2 indicates that CSDs have a relative narrow distribution pattern with no long term tail in both large garnet and small garnet bearing schists indicating LSW type distribution function. Nevertheless, the discrepancy of CSDs from LSW function can be found in large grain sizes from 1.5 Rm to 3.0 Rm. This discrepancy is also shown in CSDs obtained by Cashman & Ferry (1988) and Miyazaki (1991).

The density of grains in large-garnet bearing schists is very small compared with that in small-garnet bearing schists. The number density gradually decreases in the boundary zone between large- and small-garnet bearing schists. The modal compositions of muscovite, hornblende, albite (oligoclase), quartz and biotite are similar in these rock types. Furthermore, the Fe/Mg ratio in both rock types is similar. It is concluded from this that the chemical composition of rocks does not control the grain size of garnet. The CSDs of basic schists are similar to those of pelitic schists as mentioned above, suggesting similar growth process in large and small grains of garnet studied here.

Representative chemical compositions of garnet are listed in Table 1. As described in Banno et al. (1986), chemical compositions of the core of large grains of garnet are the same as those of small grains, and the compositions of the rim are also the same in grains of various sizes. Thus average growth velocity is largely different even in homogeneous pelitic schists

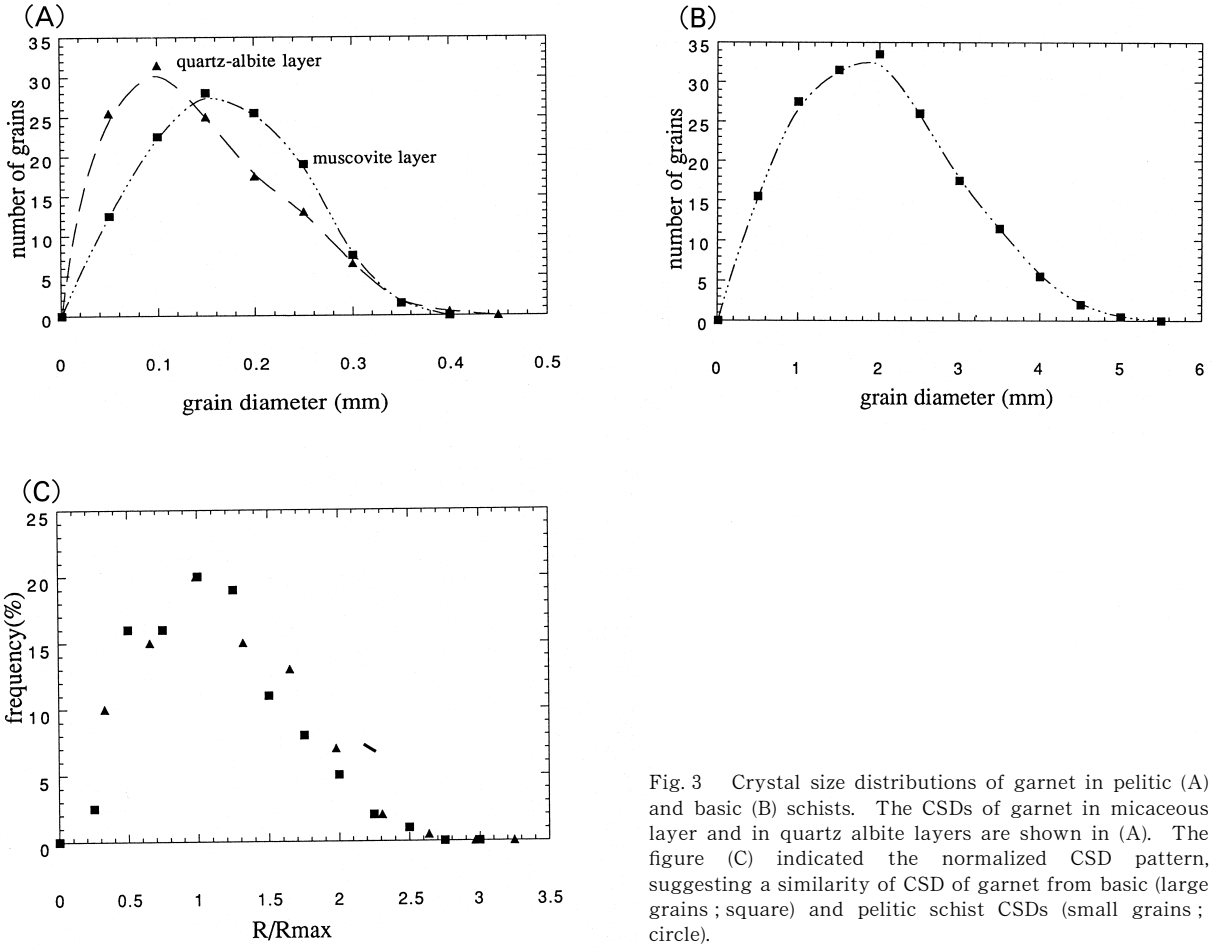

Fig. 3 Crystal size distributions of garnet in pelitic (A) and basic (B) schists. The CSDs of garnet in micaceous layer and in quartz albite layers are shown in (A). The figure (C) indicated the normalized CSD pattern, suggesting a similarity of CSD of garnet from basic (large grains ; square) and pelitic schist CSDs (small grains ; circle).

Table 1 Representative analyses of garnet cores, mid-regions and rims.

	q36PBGrim	q36PBGint	q36PBGcore	q36P1Grim	q36P1Gint	q36P1Gcore
SiO2	37.5	37.37	37.74	37.51	37.29	37.31
Al2O3	21.21	21.06	20.83	20.58	20.76	20.76
TiO2	0.11	0.09	0.04	0.11	0.09	0.13
FeO	29.01	28.65	28.23	30.26	27.07	23.95
MnO	0.58	1.29	2.89	0.36	2.39	6.88
MgO	2.19	1.78	1.52	2.58	1.41	0.63
CaO	8.57	9.14	8.53	8.04	10.29	10.42
total	99.17	99.38	99.78	99.44	99.3	100.08

*rim; rim of garnet, int; intermediate of garnet, core; core of garnet.

within a 2.5 m distance : large grains formed by large growth velocities, and small garnet grains represent small growth velocities.

The apparent increase of garnet growth velocity with increasing grain size has been described by Sakai (1985) and Banno et al. (1986) in the Sambagawa metamorphic belt from single sections based on zonal structures. All grains of garnet in single rock samples have a similar compositional trend from the core to the rim as shown in Fig. 4. This fact indicates that small grains did not experience any resorption. Considering the presence of chlorite in studied garnet bearing schists, the LSW type CSDs are not attributed to post-growth annealing. Therefore, CSD patterns in such samples may be derived from growth processes rather than Ostwald type post growth annealing.

Mean sizes of garnet grains are locally variable even in a single hand specimen. The CSDs

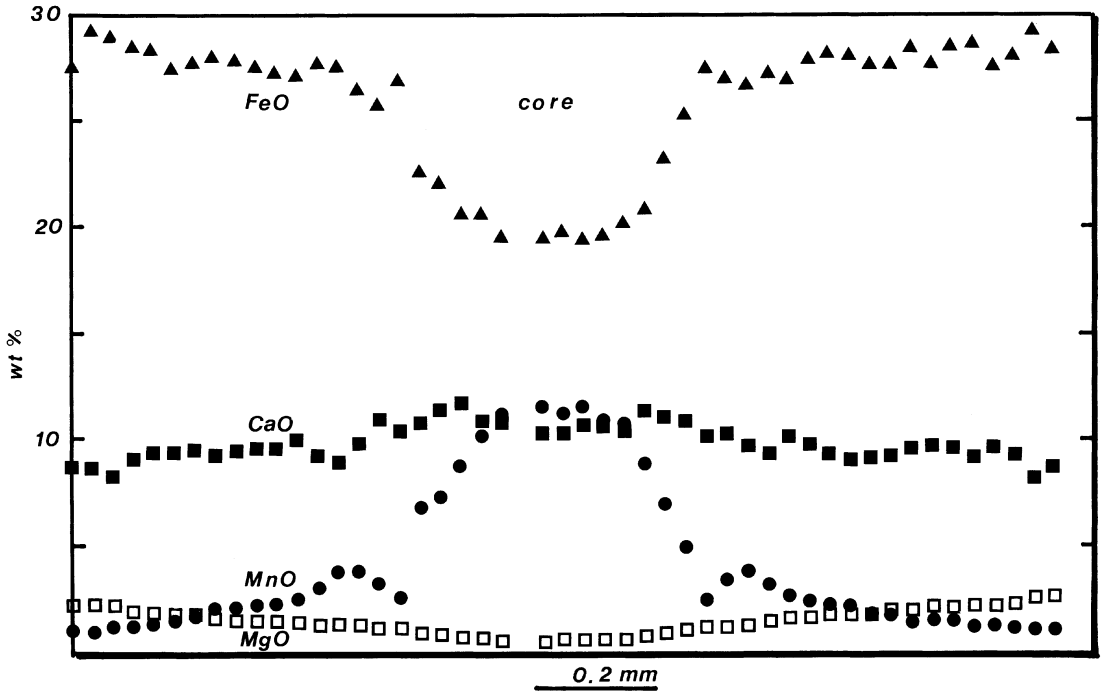

Fig. 4 Compositional zoning of garnet in q36B, indicating a gradual increases of MgO toward the rim and reverse zoning of MnO in the outer layer of garnet.

depend on local mineral compositions. In micaceous layers large grains are dominant, although small and large grains are present in quartz-albite layers. Grain sizes are apparently dependent on the mean spacing between garnet grains : the distance between small grains is commonly small and that of large grains is large. The relations between local spacings and grain sizes of garnet are shown in Fig. 5, suggesting a linear relation between them. It follows that small garnet grains tend to form in a cluster and large grains tend to be more isolated.

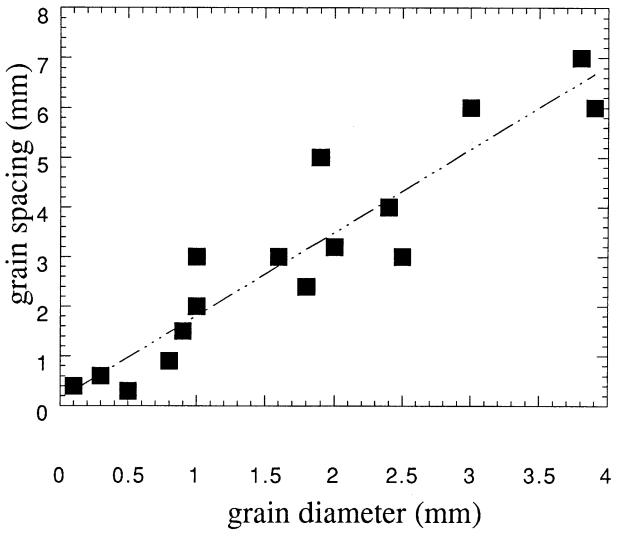

Fig. 5 Relationship between average grain size and mean spacing to neighbouring five grains. This suggests that grain spacing is proportional to grain size.

Grain size and reverse zoning of garnet

Chemical zoning of representative garnet grains Sambagawa samples are shown in Fig. 6. The MnO content decreases, and the FeO content increases from the core to the rim of garnet in pelitic and basic schists. The CaO content in pelitic schists increases from the core to the intermediate region and decreases again to the rim. The core composition of small grains are similar to those of relatively large grains, as described by Sakai et al. (1986). Sakai et al. (1986) attributed this to growth velocity being proportional to the grain radius.

Zoning profiles of analysed garnet grains are characterized by MnO enrichment at the core of grains although MgO increases gradually from the core to the rim. The pattern of MnO enrichment appears that the MnO content increases rapidly and again decreases gradually outward as shown in Fig. 4. The outline of iso-MnO content at the beginning of MnO enrichment (reverse zoning) can be found by Xray mapping

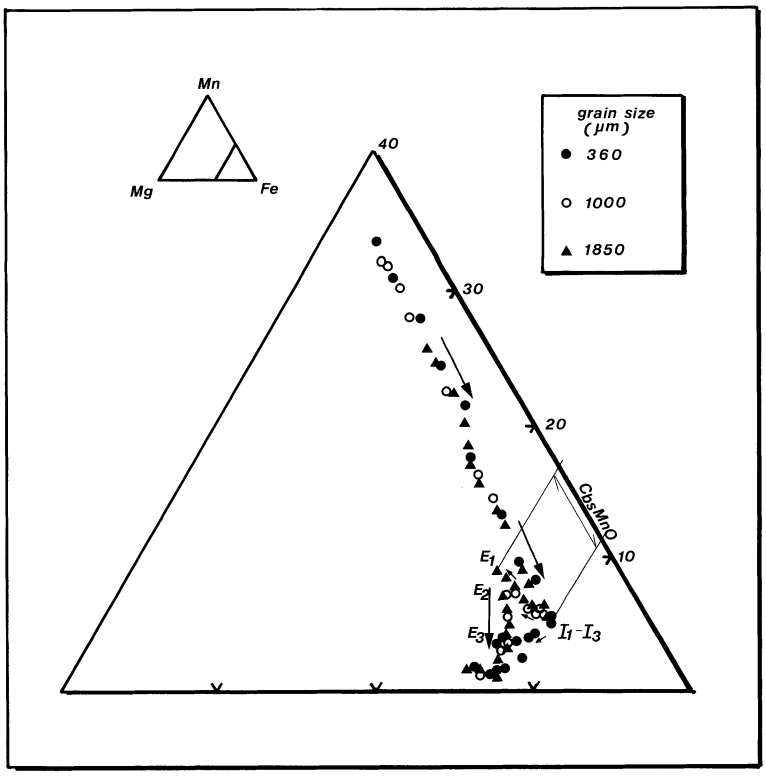

Fig. 6 Compositional paths of garnet in sample q 36P1 in Mn-Fe-Mg diagram. The initiation and cessation points of the reverse zoning of grains are shown by I1-I3 and E1-E3, respectively. This shows that the large grain indicates markedly reverse zoning. The intensity of reverse zoning is defined as the difference of MnO content from I to E, and is indicated by Cbs MnO.

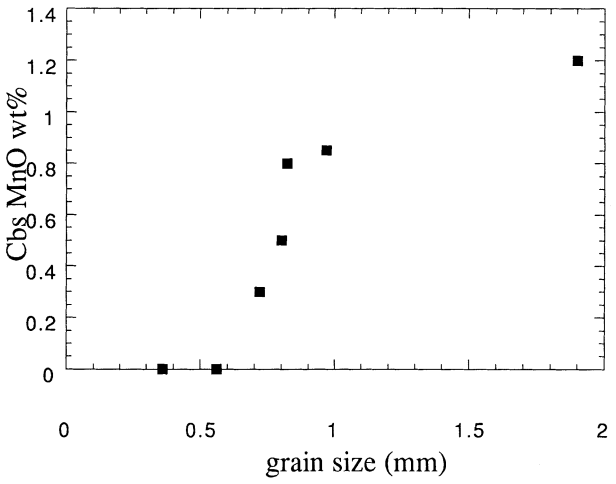

Fig. 7 Relationship between compositional difference Cbs in MnO from the initiation to the cessation points of the reverse zoning and grain size of garnet.

(CMA mapping) using automatic XMA. The representative CMA image of the reverse-zoned garnet is shown in Fig. 8. It is apparent that the outline of the beginning of the reverse zoning is consistent with the growth surface outlined by {110}. Therefore, the reverse zoning is not due to resorption of garnet as suggested by Kretz (1973) and Banno & Chii (1978), but rather resulted from growth processes.

The reverse zoning of MnO content is found in large grains of garnet, but not in small grains. In addition, the difference of MnO content between the beginning of the reverse zoning and the middle part of the reverse zone in a single garnet increases with increasing grain size. The relationship between the compositional range of the MnO content (hereafter called as backstep composition of MnO) of the reverse zoning and grain size is shown in Fig. 7. The MnO-backstep content shows an asymptotic relationship to grain size. The relationship between the MnO-backstep and the grain size in basic schists is similar to that in pelitic schists.

Discussion

1. Growth of garnet in clusters

Cashman & Ferry (1988) and Miyazaki (1991) interpreted garnet growth in metamorphic rocks and resultant LSW type pattern of crystal size distribution (CSD) in terms of Ostwald ripening of garnet. Ostwald ripening requires that the growth velocity depends on the interfacial energy between garnet and surrounding matrix minerals. In this process, the growth velocity of small grains is negative and that of large grains is positive. However, continuous zonings of MnO, FeO and MgO suggests that

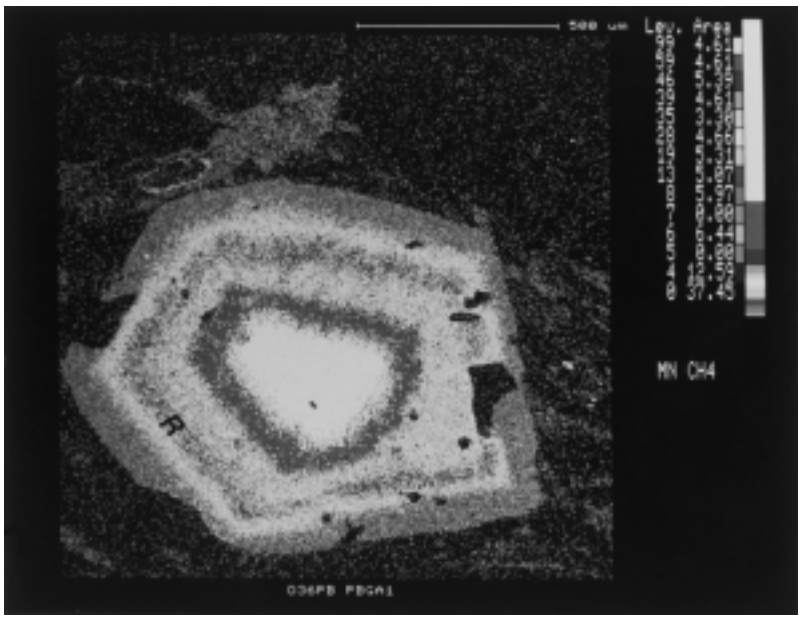

Fig. 8 Mapping of MnO content in the reversely zoned garnet from q36PB sample in Fig. 2. the band of the reverse zoning is marked by R.

selective resorption of small garnet cannot be found in either pelitic or basic schists. Consequently, the Ostwald ripening might not operate strongly on the growth of garnet due to consumption of chlorite and quartz.

The kinetics of diffusion of the component ions of garnet in matrix chlorite and reaction at the growth surface of garnet is considered here. The system has multigrains in the core region of the diffusional field concerning component ions of garnet. In the diffusional field, where the number of garnet grains is n and the average grain size is R, we have the following mass balance equation ;

$$4n\pi R^2 dR/dt = 4\pi r^2 D dc/dr \quad (1)$$

in which c and D are the concentration of component ions at the distance r from the cluster center and diffusion constant of the slowest component ion of garnet and chlorite in the matrix, respectively. Integrating this equation at the boundary conditions of

$$c = c_o \text{ at } r = \text{infinite} \quad (2)$$

and

$$c = c_{oo} \text{ at } r = R \text{ (growth surface)} \quad (3)$$

we have

$$\delta C = n\ R\ V/D \quad (4)$$

where $V = dR/dt$ and $\delta C = c_o - c_{oo}$. Then $2RdR/dt$ becomes dR^2/dt. Therefore, we obtain the average growth velocity Vm

$$V_m = (1/t)\int V(t)dt = R/t = (2\delta C\ D/t)^{1/2}\ n^{-1/2}. \quad (5)$$

Furthermore, according to eqn. (5), the relationship between the average spacing and the grain size of garnet can be inferred as follows ;

$$R = \{\delta C^{1/2}(l/L^{1.5})\}\ d^{1.5} \quad (6)$$

in which l is the diffusional length of component ions during growth of garnet ($l^2 = 2Dt$) and L is the scale of a garnet cluster as defined by

$$n\ d^3 = L^3. \quad (7)$$

As shown in Fig. 5, the mean spacing of garnet grains is proportional to the grain size of garnet and the ratio of $d^{1.5}/R$ is about 3.0–4.0. Considering $\delta C = 0.01$, l reaches about 2–5 times of L, indicating that the scale of the diffusional field is larger than that of the cluster.

2. A model of reverse zoning

Kretz (1973) and Banno & Chii (1978) attributed the reverse zoning of garnet to the retrograde growth of garnet and the difference between the equilibrium composition of chlorite at the growth surface and the average composition far from the growth surface. Unless the equilibrium composition exists at the growing surface both in reactant chlorite and product garnet, the growth of garnet during decreasing temperature and/or pressure requires excess Mn chlorite relative to the equilibrium composition at peak pressure (Fig. 9). Reverse zoning resulting from the retrograde growth of garnet should then continue until the average composition of chlorite is equal to the equlibrium one (at point r in Fig. 9). Then, the MnO backstep magnitude is governed by the average composition of

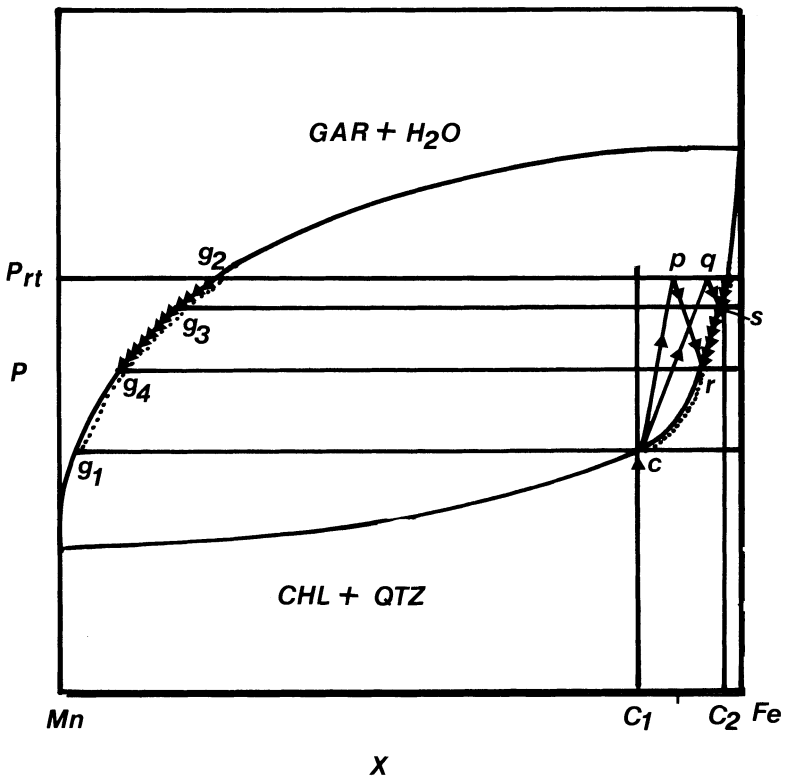

Fig. 9 Proposed growth model of reversely zoned garnet in the system garnet-chlorite-biotite-muscovite-quartz-H 2 O at the high pressure conditions. The equilibrium compositions of garnet and chlorite at their interfaces are assumed, and thus the reverse zoning of garnet requires a decrease in pressure because continuous enrichment of MgO in garnet in reverse zoning indicates pressure increase at this stage. G ; garnet, c-p-r ; pathe of bulk chlorite composition in the case of fast growth velocity, c-q-s ; pathe in the case of slow growth velocity of garnet (see text).

matrix chlorite at the turning pressure to the retrograde metamorphism.

Consider a simple model in which average compositions of the matrix chlorite are represented by a simple average of chemical composition in the diffusional field and its exterior region. The diffusional length can be obtained by diffusion equation with moving boundary between chlorite and growing garnet in the spherical coordinates. Assuming the velocity of boundary migration due to garnet growth Vm, we have the following differential equation,

$$D\, d^2c/dr^2 + V_m\, dc/dr = 0 \qquad (8)$$

In solving this equation, we have a specific solutions near the growth front as follows ;

$$c(r) = \exp(-V_m\, r/D). \qquad (9)$$

Thus, the diffusional length L around a single garnet can be defined by

$$c(L) = c_{oo}\, e^{-1}.$$

Therefore, we obtain

$$k = D/V_m \qquad (10)$$

The diffusional field has a volume surrounding a single garnet grain of

$$v_r = 4/3\,\pi k^3. \qquad (11)$$

On the other hand, the matrix volume surrounding a single grain of garnet represents

$$v = N^{-1} \qquad (12)$$

in which N is the population density of the garnet grain (cm^{-3}). Consequently, the average compositions, x, of diffusional field and its exterior region surrounding a garnet grain becomes

$$x = (C_1(v\text{-}v_r) + C_2 v_r)/v \qquad (13)$$

in which C_1 is the initial MnO content in chlorite and C_2 is the equilibrium MnO content in chlorite (see Fig. 9) at the beginning of the retrograde metamorphism.

The magnitude of the MnO backstep is considered to be proportional to the difference between the equilibrium and the average MnO contents of chlorite as illustrated in Fig. 9. Thus, we obtain

$$\begin{aligned} C_{bs} &= g(x\text{-}C_2) \\ &= g(C_1 - C_2)(1 - v_r/v) \\ &= g\,\Delta C(1 - 4\pi N D t^3/3\,R^3) \end{aligned} \qquad (14)$$

in which ΔC is the difference between C_1 and C_2, g is a constant, and t is the time of growth, which is constant in a single hand specimen. The backstep compositions C_{bs} should be zero if the value in the blanket of the above equation is smaller than zero. Thus, we obtain

$$v_r/v \sim 1 \qquad (15)$$

Then

$$D \sim V_m\, d, \qquad (16)$$

Further, if we observe R_c at $C_{bs} = 0$ as shown in

Fig. 8, we obtain the growth time of garnet, t_g to be

$$t_g = R_c\, d/D \quad (17)$$

where d is the mean spacing of garnet grains defined earlier. And, the average growth velocity of garnet becomes,

$$V = R_c/t_g = D/d. \quad (18)$$

These relations between grain size and backstep magnitude are shown in Fig. 8. The binary loops of the Mn-Fe garnet system are approximately box type because enthalpy change accompanied with this reaction is very large (Banno et al., 1986). Then, C_2 is very small so that ΔC is approximated to be C_1. As shown in Fig. 9, the MnO backstep contents seem to converge to 1.3 wt % which will be g C_1. If g is about 10, then C_1 becomes 0.1 wt % which is near the average MnO content in chlorite zone chlorite (Higashino et al., 1981). From eqn. (17), using Rc = 0.01 cm, d = 1 cm and $D = 10^{-16}$ cm^2/sec, we obtain $t_g = 10^{14}$ sec, suggesting that the model is reliable. Further, average growth velocity is about 10^{-16} cm/sec.

Conclusion

Grain sizes of garnet in higher grade pelitic and basic schists of the Sambagawa high pressure metamorphic belt vary from 0.01 to 10 mm within a single outcrop, and the CSD is similar to the LSW pattern. The local mean spacing of garnet grains increases with increasing local average of grain size, suggesting that grains in clusters create a competitive environment for the component ions of garnet from matrix chlorite around the cluster. Furthermore, large garnet grains display distinct reverse zoning of MnO, which is not apparent in small garnet grains. The ranges of MnO content in reversely zoned garnet increases asymptotically with increasing grain size.

The growth model presented here is based on the mass balance equation in the case of clustered grain growth of small garnet and the length scale is defined by the ratios of the diffusivity of component ions in matrix chlorite and the mean grain growth velocity of garnet. In addition, the model requires surface equilibrium at the interface between chlorite and garnet in the case of reverse zoning, and thus reverse zoning formed during decrease of pressure under isothermal conditions. The growth model presented here is consistent with the relationship between grain size and population densities of grains, and the relationship between the magnitude of reverse zoning of MnO and grain size.

Acknowledgements

The authors thank Tadao Nishiyama and Aaron Stallard for critical reviews.

Reference

Banno, S. and Chii, S., 1978, A model to explain the Mn enrichment in the rim of zoned garnet. *Geochem. J,* **12**, 253–257.

Banno, S. and Sakai, C., 1990, Geology and metamorphic evolution of the Sambagawa belt, Japan. In : (eds.) Daly, J.S., Cliff, R.A. & Yardley, B.W.D., Evolution of Metamorphic Belts, Geol. Soc. Special Pub., **43**, 519–532.

Banno, S., Sakai, C. and Higashino, T., 1986, Pressure-temperature trajectory of the Sambagawa metamorphism deduced from garnet zoning. *Lithos,* **19**, 51–63.

Carlson, W.D., 1989, The significance of intergranular diffusion to the mechanisms and kinetics of porphyroblast crystallization. *Contrib. Mineral. Petrol.,* **103**, 1–24.

Cashman, K.V. and Ferry, J.M., 1988, Crystal size distribution (CSD) in rocks and the kinetics and dynamics of crystallization. III. Metamorphic crystallization. *Contrib. Mineral. Petrol.,* **99**, 401–415.

Hara, I., Shiota, K., Hide, K., Okamoto, K., Takeda, K., Hayasaka, Y., and Sakurai, Y., 1990, Nappe structure of the Sambagawa belt. *J. Metamorphic Geol.,* **8**, 441–456.

Higashino, T., 1990, The higher grade metamorphic zonation of the Sambagawa metamorphic belt in central Shikoku, Japan. *J. Metamorphic Geol.,* **8**, 413–424.

Higashino, T., Sakai, C., Otsuki, M., Itaya, T., and Banno, S., 1981, Electron microprobe analyses of rock-forming minerals from the Sanbagawa metamorphic rocks, Shikoku, Part 1 Asemi river area. *Sci. Rept. Kanazawa Univ.,* **26**, 73–122.

Hollister, L.S., 1966, Garnet zoning : An interpretation based on the Rayleigh fractionation model. *Sci-*

ence, **154**, 1647–1651.

Itaya, T. and Takasugi, H., 1988, Muscovite K-Ar ages of the Sambagawa schists, Japan, and argon depletion during cooling and deformation. *Contrib. Mineral. Petrol.,* **100**, 281–290.

Kretz, R., 1973, Kinetics of the crystallization of garnet at two localities near Yellowknife. *Can. Mineral.,* **12**, 1–20.

Kurata, H. and Banno, S., 1974, Low-grade progressive metamorphism of pelitic schists of the Sazare area, Sanbagawa metamorphic terrain in central Shikoku, Japan. *J. Petrol.,* **15**, 361–382.

Miyazaki, K., 1991, Ostwald ripening of garnet in high P/T metamorphic rocks. *Contrib. Mineral. Petrol.,* **108**, 118–128.

Mori, K., 1986, Plastic deformation and metamorphism of the Sambagawa and Shimanto belts in Kii Peninsula, central Japan. Ms thesis of Ehime University.

Nomizo, A., 1989, Petrology of the Sambagawa metamorphic rocks in the Saijo area, central Shikoku, Japan. Ms thesis of Univ. Tokyo.

Nomizo, A., 1992, Three types of garnet in a Sambagawa pelitic schist near the Sebadani eclogite mass, central Shikoku, Japan. *J. Geol. Soc. Japan,* **98**, 49–52.

Sakai, C., 1985, Metamorphism and deformation of the Sanbagawa metamorphic terrain, central Shikoku. PhD thesis of Kyoto University.

Sakai, C., Banno, S., Toriumi, M. and Higashino, T., 1985, Growth history of garnet in pelitic schists of the Sanbagawa metamoprhic terrain in central Shikoku. *Lithos,* **18**, 81–95.

Spear, F.S., and Peacock, S.M., 1989, Metamorphic Pressure-Temperature-Time Paths. Short Course in Geology, volume 7, American Geophysical Union.

St-Onge, M.R., 1987, Zoned poikiloblastic garnets : P-T paths and syn-metamorphic uplift through 30 km of structural depth, Wopmay orogeny, Canada. *J. Petrol.,* **28**, 1–22.

Takasu, A., 1989, P-T histories of peridotite and amphibolite tectonic blocks in the Sanbagawa metamorphic belt, Japan. *In* Daly, J.S., Cliff, R.A., and Yardley, B.W.D., eds., *Evolution of Metamorphic Belts*, Geol. Soc. Special Pub., **43**, 533–538.

Takasu, A. and Dallmeyer, R.D., 1990, 40 Ar/39 Ar mineral age constraints for the tectonothermal evolution of the Sambagawa metamorphic belt, central Shikoku, Japan : A Cretaceous accretionary prism. *Tectonophysics,* **185**, 111–139.

Tracy, R.J., 1982, Compositional zoning and inclusions in metamorphic minerals. *In* Ferry, J.M., ed., *Characterization of Metamorphism through Mineral Equilibria*, Mineral. Soc. Am. Rev. Mineral., **10**, 355–397.

Toriumi, M., 1975, Petrological study of the Sambagawa metamorphic rocks, Kanto Mountains, Japan. *Bull. Univ. Museum Univ.* Tokyo, **9**, 1–99.

Toriumi, M., 1982, Strain, stress and uplift. *Tectonics,* **1**, 57–76.

Toriumi, M., 1989, Microstructures of regional metamorphic rocks. *In* Karato, S. and Toriumi, M., eds., *Rheology of Solids and of the Earth*, Oxford Univ. Press, 319–337.

Toriumi, M., 1990, The transition from brittle to ductile deformation in the Sambagawa metamorphic belt, Japan. *J. Metamorphic Geol.,* **8**, 457–466.

Vance, D. and O'Nions, R.K., 1992, Prograde and retrograde thermal histories from the central Swiss Alps. *Earth Planet. Sci. Lett.,* **114**, 113–129.

Wallis, S. and Banno, S., 1990, The Sambagawa belt-trends in research. *J. Metamorphic Geol.,* **8**, 393–400.

Wallis, S., 1991, Vorticity analysis in a metachert from the Sanbagawa Belt, SW Japan. *J. Struct. Geol.,* **14**, 271–280.